2011 NDIA GROUND VEHICLE SYSTEMS ENGINEERING AND TECHNOLOGY SYMPOSIUM
MODELING & SIMULATION, TESTING AND VALIDATION (MSTV) MINI-SYMPOSIUM
AUGUST 9-11 DEARBORN, MICHIGAN

UTILIZING SIMULATION TECHNOLOGY FOR IMPROVING OCCUPANT SURVIVABILITY FOR A VEHICLE SUBJECTED TO LOADS FROM EXPLOSIONS

Nickolas Vlahopoulos
Department of Naval Architecture and Marine Engineering
University of Michigan
Ann Arbor, MI

Geng Zhang
Michigan Engineering Services, LLC
Ann Arbor, MI

ABSTRACT

The Blast Event Simulations sysTem (BEST) is a synthesis tool that provides a seamless and easy-to-use coupling between existing and commercially available LS-DYNA solvers and Anthropomorphic Test Device (ATD) models for a complete sequence of explosive simulations. BEST driven simulations capture the soil/explosive/vehicle/occupant interaction. In this paper a blast simulation analysis conducted by BEST for a generic but representative vehicle is presented. The vehicle is subjected to the blast load created by an explosive buried underneath the vehicle. An ATD model is placed inside the vehicle in order to capture the loads created on the lower legs of an occupant due to the explosion. Technical details with respect to the various models engaged in the simulation are presented first. The results and the physical insight which can be gained by the analysis are discussed. A series of design modifications which add minimal weight are introduced in the vehicle structure, such as using rigid polyurethane foam material, introducing a foot rest, adding a rail stiffener on the floor, and various combinations of these design alternatives; the effects of the design changes on the forces generated on the legs of the occupant are identified through simulation. The results are analyzed in order to gain a physical insight about the design changes which improve survivability. The material presented in this paper demonstrates how simulations can be used for increasing occupant survivability and for understanding the physics which are critical for mitigating occupant injury.

INTRODUCTION

The design of vehicles to resist a blast and provide protection to the vehicle and its occupants is of great interest. New combat vehicle designs emphasize weight reduction for increased fuel efficiency and airborne transportation; therefore, a significant effort must be invested to ensure that the vehicle's survivability is not compromised.

In the past, several efforts have been made for modeling explosions and their effect on structures [1-4]. Empirical loading models have also been developed for predicting the effects of blast mines on structures. Empirical blast loading functions were implemented in the CONWEP code [5] for modeling the free air detonation of a spherical charge. Another empirical relationship was developed for predicting the impulse applied by a buried mine to a plate at a given offset from the mine [6]. Both empirical models were integrated with the LS-DYNA commercial code. The CTH hydrocode [7,8] has been developed by Sandia National Laboratories and utilized for blast event simulations in multiple occasions for modeling blast events.

In this paper, the Eulerian solver of LS-DYNA is employed for simulating the soil – explosive – air interaction and calculating the loads on a target structure. Sequentially, the LS-DYNA Langragian solver is used for computing the corresponding response of a target structure to the loads from the explosion. A major advantage of utilizing the LS-DYNA solvers for blast event simulations instead of CTH is that LS-DYNA is a commercially readily accessible software, has a friendly user interface, it can exchange data with commercial pre and post processors, it is easy to interpret the structure of its data file, and numerical models for an ATD can be readily integrated in the simulation as part of the vehicle finite element model.

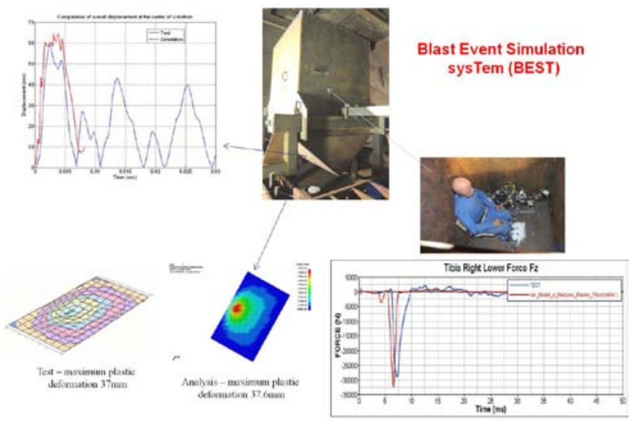

Figure 1. Comparison between results from BEST and test data for a V shaped double bottom structure and the enclosed occupant (from [9])

The BEST user interface has built-in knowledge for preparing the various data files required for conducting the blast simulation and ADT analysis. In this manner, it eliminates the burden of specialized knowledge from the analyst who will be conducting the simulations. BEST results have been validated through comparison to test data [4, 9] and a brief summary from [9] is presented in Figure 1.

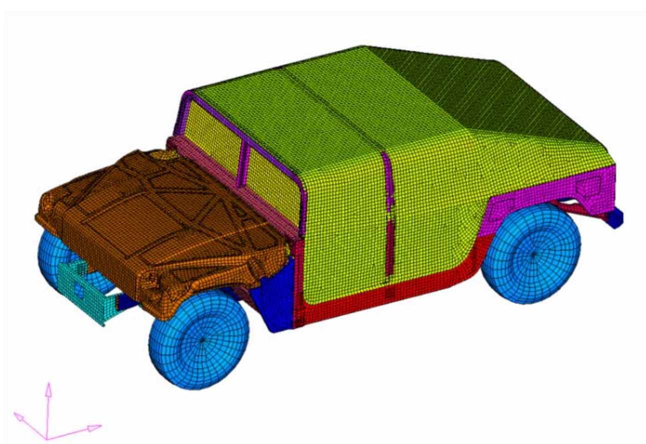

Figure 2. FEA model of a generic vehicle used in the study presented in this paper

In this paper, a vehicle study conducted through BEST is presented. A vehicle and occupant response simulations to non-centerline buried explosive were conducted. The Finite Element Analysis (FEA) model of a generic vehicle is presented in Figure 2. Although the geometry is representative, the material properties and the thicknesses of the various components are generic.

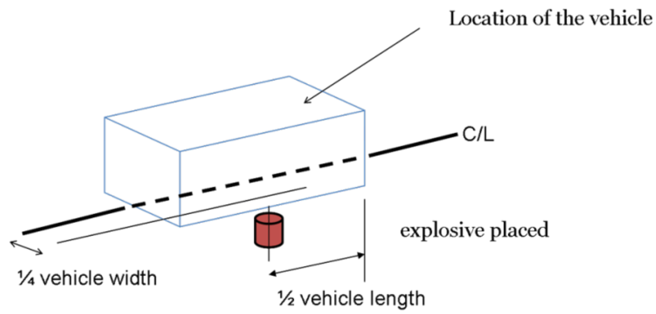

Figure 3. Relative placement of explosive with respect to the vehicle

The relative location of the explosive to the vehicle is depicted in Figure 3. The explosive is 6 kg of C4 buried with 5cm distance between the top of the soil and the top of the explosive. From front to back, it is right under the center of the vehicle. From left to right, it is ¼ width away from the left side of the vehicle. The BEST process is used to conduct the simulations. Several blast mitigation alternatives were studied for reducing the loads developed in the legs of the occupant. Firstly design changes were considered for the floor of the vehicle in order to reduce the deformation of the floor. This was pursued since the deformation of the floor provides the loading for the legs of the occupant, thus a smaller floor deformation is expected to have a positive impact on the loads developed in the occupant's legs. Not including the model for the ATD makes the simulations faster and thus a larger number of alternatives can be considered during the initial screening process. A floor configuration with a sandwich type of structural panel with rigid polyurethane foam material in between the outer steel panels was identified as a useful blast mitigation strategy. Then an ATD model was included in the simulations and a further refinement of the design was pursued for reducing the forces developed in the legs of the occupant. A combination of a foot-resting panel and of a stiffening rail provided the best reduction in the loads. This design study demonstrated how it is possible to use the BEST process as mitigation of blast injuries through modeling and simulation.

COMPUTING THE LOADS FROM THE EXPLOSION

The first step of the simulation process is to use BEST to automatically generate the Air/Explosive/Soil model based on the geometry of the vehicle and on user's input about the placement of the explosive, and the space around the vehicle where the air model and the soil model will be created. The model created for the vehicle application presented in this paper is depicted in Figure 4. The BEST code automatically eliminates the air (grey color) elements from locations occupied by the vehicle. It also automatically creates tracer point locations at air elements interfacing with the vehicle for recording the blast pressure histories from the Eulerian analysis and transferring them as loading to the Lagrangian vehicle analysis.

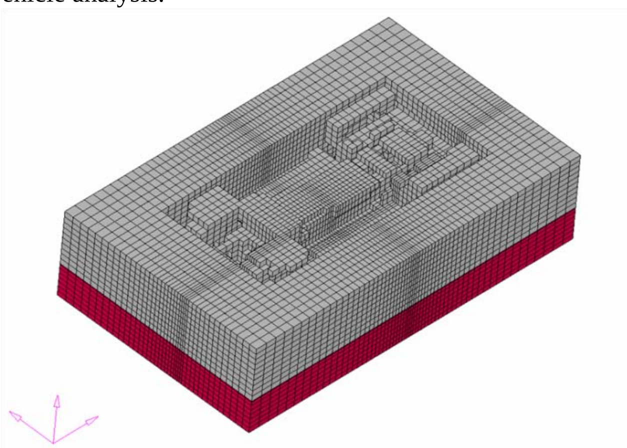

Figure 4. Model for the Air/Explosive/Soil used in the vehicle analysis presented in this paper

The LS-DYNA Eulerian solver is used for conducting the analysis which creates the loads applied on the vehicle from the explosion. Representative results from the LS-DYNA analysis showing the soil ejected from the explosion and the hole created in the soil from the explosion are presented in Figure 5.

Figure 5. Crater created in the soil from the explosion and soil ejected in the air

For the work presented in this paper, the Eulerian simulation is carried out for 10 milli-seconds. Typical pressure histories for a few representative tracer points are presented in Figure 6. As it can be observed, the pressure peaks are reached within less than 1 milli-second and after 2 milli-seconds the pressure loading becomes very small. The latter demonstrates that although the air and soil models are limited in the vicinity of the vehicle, due to the short duration of the simulated time and the boundary conditions used in the simulations there are no reflection effects that would reload the pressure on the structure after the initial peak pressure loads from the explosion have been encountered.

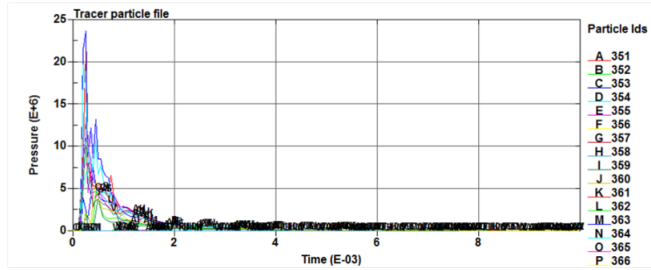

Figure 6. Pressure time histories at representative tracer points

COMPUTING THE RESPONSE OF THE VEHICLE

The computed pressure loading is then applied on the vehicle model. BEST uses the pressure time histories at the tracer points for generating the input loading for the Lagrangian LS-DYNA vehicle analysis. In the baseline vehicle configuration the thickness of the floor is 6mm and the material is steel. Figure 7 presents the deformation induced on the floor at the instant of time when the largest deformation is encountered. The side doors and the roof are removed from the model display when generating Figure 7 in order to make the deformation of the floor visible.

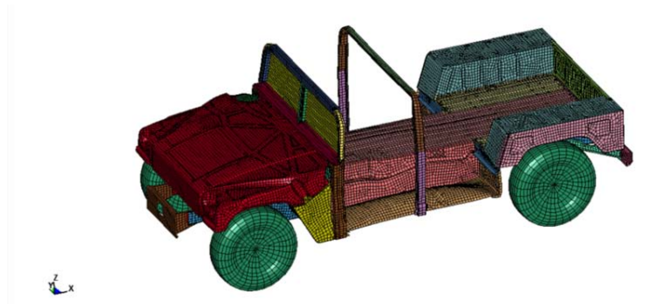

Figure 7. Deformation of the floor for the baseline vehicle configuration

The left side floor experienced large deformation, but no significant damage. The LS-DYNA did report certain number of elements being destroyed, which is an indication of cracks or perforations at local regions, but overall the floor is in good integrity and suitable for future placement of dummy models inside the vehicle. This configuration provides the starting point for the design analysis that identifies blast mitigation strategies which reduce first the deformation on the floor of the vehicle, and thus the forces developed on the occupant. With 6mm floor, the total mass of the baseline vehicle design is 4286.86 Kg.

BLAST MITIGATION ALTERNATIVES FOR REDUCING THE FLOOR DEFORMATION

Before introducing the model of the ATD in the simulations, blast mitigation strategies were evaluated for reducing the deformation on the floor. These computations are conducted faster compared to the ones that include the ATD, so they are used during an initial screening of the alternative blast mitigation strategies. Figure 8 depicts just the floor and a node placed in the location of the interface between the occupant and the floor where the deformation will be monitored for determining the effectiveness of the blast mitigation strategy.

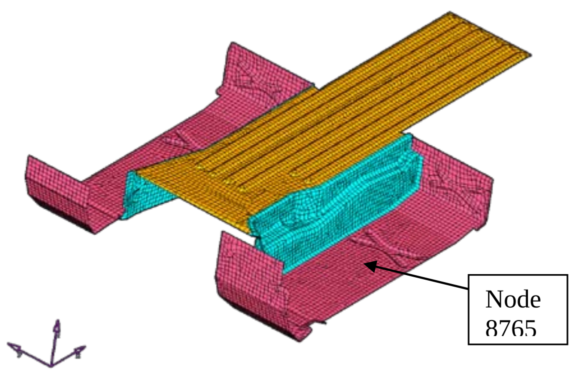

Figure 8. Initial design of vehicle floor (6mm) and location of node where the deformation is monitored for assessing the effectiveness of the blast mitigation strategy

Several alternative designs were considered in an effort to reduce the maximum deformation on the floor at the monitored location. Results from two of the alternatives are presented in this Section. The first option is to add a layer of Rigid Polyurethane Foam (RPF) material to the outer bottom surface of the floor. RPF material is considered in published work on blast mitigation strategies as a good material for absorbing blast energy and mitigating structural damage [10, 11]. The RPF material is modeled with solid elements, it is considered to have thickness of 2cm and added 10.45 Kg to the mass of the vehicle.

The BEST code is used to reconstruct the air/explosive/soil model since the outer geometry of the vehicle structure changed. Then the Eulerian analysis is conducted to obtain the new blast pressure and the Lagrangian analysis is repeated to obtain the new vehicle response. Since the vehicle had an initial ground clearance of 40 cm and the PRF material is only 2cm thick, the new blast pressure is higher by a small amount compared to the old blast pressure. However, the deformation at the vehicle floor has been reduced due to absorption of blast energy by RPF material. The vertical displacement of node 8765 at the floor is presented in Figure 9 for the initial design of uniform 6mm thickness and in Figure 10 for the new design with RPF added at the outer bottom surface of the floor. With the design modification, the maximum displacement of node 8765 is reduced from 17.5 cm to 13.5 cm, about 23% reduction.

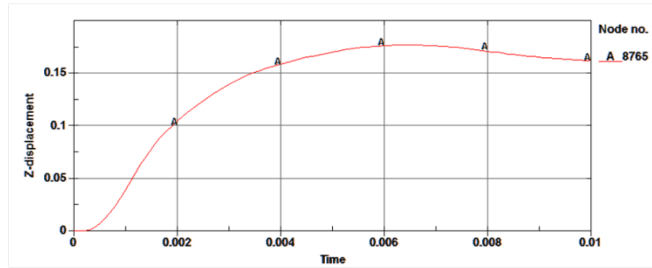

Figure 9. Vertical displacement of node 8765 at the vehicle floor, baseline design

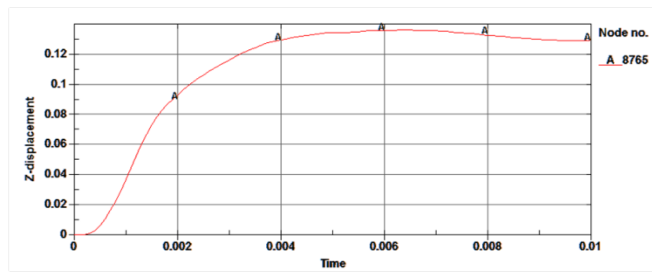

Figure 10. Vertical displacement of node 8765 at the vehicle floor, configuration with RPF added on the exterior bottom surface of the floor

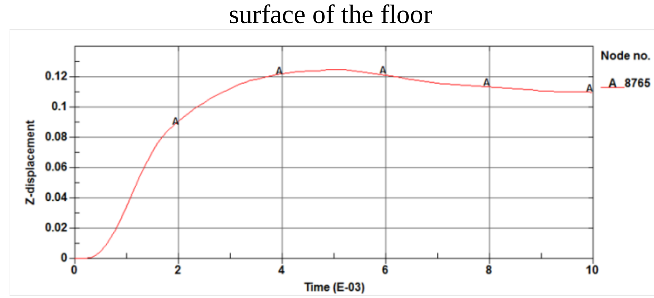

Figure 11. Vertical displacement of node 8765 at the vehicle floor, sandwich design with inner/outer floor and RPF in between

The second alternative is to split the floor into inner floor and outer floor, with RPF material placed in between the inner and outer floor. The thickness of the RPF is 2cm. The inner floor has thickness of 2mm and the outer floor has thickness of 4mm. The vertical displacement of node 8765 is shown in Figure 11. With the second floor configuration the maximum displacement is reduced even further to 12.5cm (about 29% reduction with respect to the baseline). The floor response is further reduced due to the absorption of blast energy by the RPF material and the decoupling effect that the RPF offers in the sandwich floor configuration. This configuration comprises the starting point of the design analysis which includes the ATD and evaluates blast mitigation strategies for reducing the forces in the legs of the occupant. It introduces only a small increase in the mass of the floor compared to the starting design.

ATD MODELING AND ALTERNATIVE MODELING STRATEGIES

A Humanetics (previously FTSS) dummy FEA model is used in this work to represent the ATD. Figure 12 presents the FEA model of the dummy. The dummy has about 100K nodes and 130K elements, while as a reference the vehicle has about 94K nodes and 106K elements. The FTSS dummy model has beam type load cell elements embedded inside the dummy. Response histories of the load cells are recorded for the entire simulation, later they can be extracted to plot force and moment histories at certain body locations. The FTSS dummy also has accelerometers associated with certain nodes to record acceleration histories at certain body locations. Figure 12 presents cross-sectional views of the dummy torso and leg.

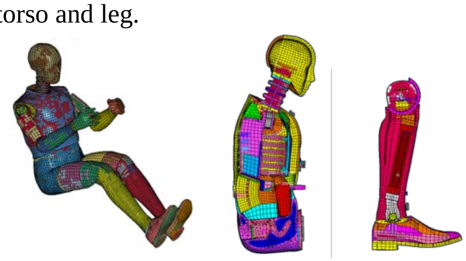

Figure 12. FEA model of ATD

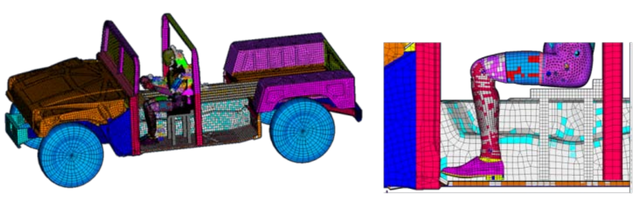

Figure 13. Dummy placement inside the vehicle

A generic seat is added into the vehicle model, and then the FTSS dummy is placed inside the vehicle. The dummy is positioned sitting upright on the seat. Effort is made to place the dummy as close as possible to the contact surface to vehicle, so that the dummy will interact with the structure as soon as the blast simulation begins. At the same time, a minimal gap between dummy and structure is retained so that there is no initial penetration. The final position of the dummy inside the vehicle is presented in Figure 13. A detailed view of the dummy feet placement is also presented in Figure 13.

A Lagrangian LS-DYNA data file is created to link the vehicle model, seat model and dummy model together. The dummy model has its own contact definition for all body parts. Additional contact is defined between structure/vehicle parts to dummy parts. The analysis is conducted by LS-DYNA, and the vertical forces at dummy's left and right tibia comprise the main metric for evaluating each blast mitigation strategy which is being considered. A comparison is made for the loads developed on the tibia locations of the dummy for the baseline floor and the sandwich floor. The results for the left upper and lower tibia are presented in Figure 14 and the results for the right upper and lower tibia in Figure 15. Due to the large size of the combined vehicle and dummy model, the solution of response up to 3 ms took 28 hours to finish on a single CPU of a DELL computer. Due to the severity of the load from the explosion the structure and the dummy are experiencing large deformation and complex contact, thus LS-DYNA has to use extremely small time step to maintain numerical stability of its solution. The simulation was conducted long enough for capturing the peak forces developed on the dummy's legs. The plot shows that although there was significant reduction in the deformation of the floor, the modified design has reduced the axial force, but only by a modest amount. Further, the loads in the lower tibia are higher compared to the upper tibia and they will comprise the main focus of the discussion in the rest of the paper.

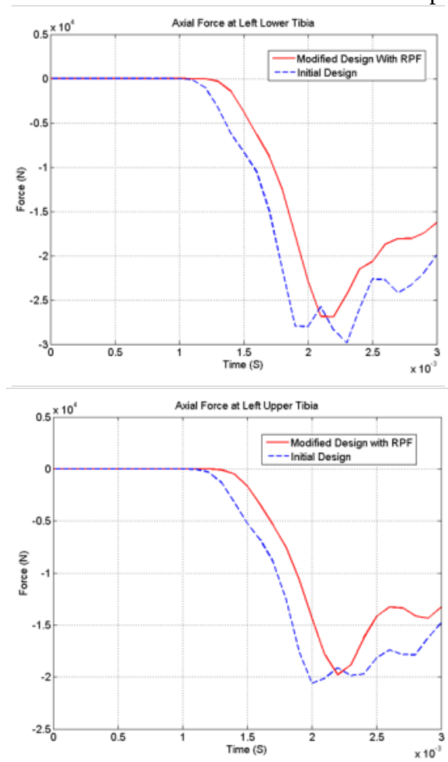

Figure 14. Axial forces at left lower tibia and left upper tibia

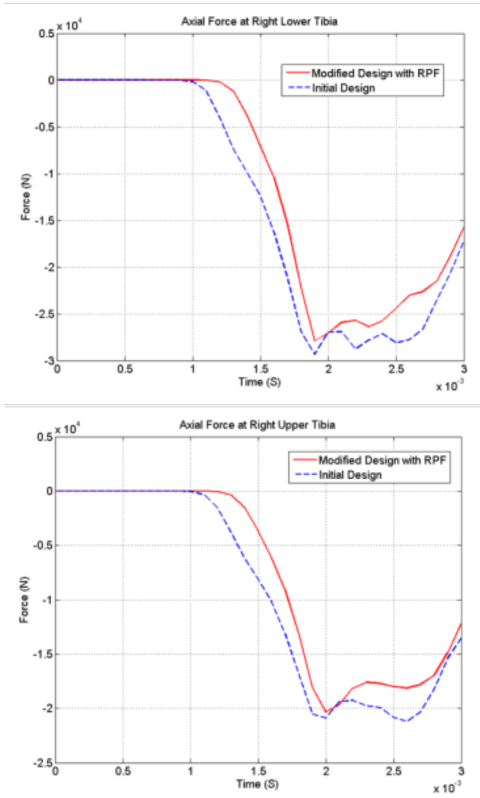

Figure 15. Axial forces at right lower tibia and right upper tibia

Before progressing in further investigating design strategies for reducing the lower tibia loads, a comparison is made between two alternative LS-DYNA solution strategies. Either a decoupled Eulerian – Lagrangian simulation process or a fully coupled Eulerian – Lagrangian simulation process can be facilitated. Since the decoupled process considers the boundary of the vehicle as rigid when computing the loads which are applied on the vehicle structure, it is expected that the deformation of the vehicle and the loads computed for the ATD will be more severe (thus more conservative) when using the decoupled analysis. In order to demonstrate the relative results produced by the two modeling approaches and the required computational time, the analysis with the vehicle and the ATD for the configuration with the sandwich floor configuration was conducted using the fully coupled Eulerian-Lagrangian approach. The coupled analysis for 3ms requires 10 days of cpu time on a single processor of a DELL computer, while the decoupled analysis requires 28 hours.

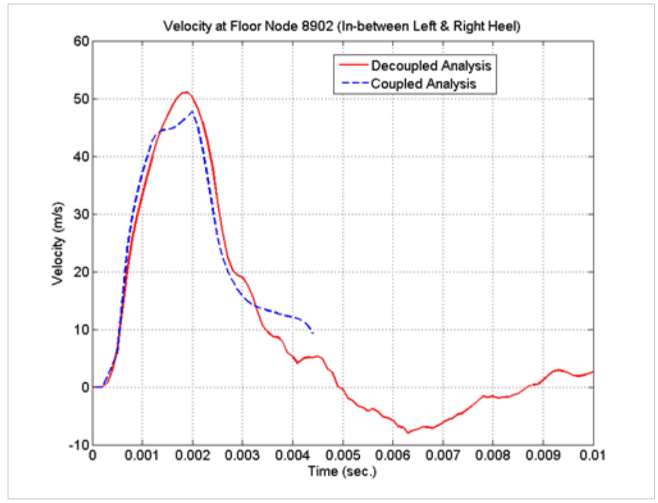

Figure 16. Velocity results from a fully coupled and from a decoupled blast simulation for the velocity at the floor in between the heels of the dummy

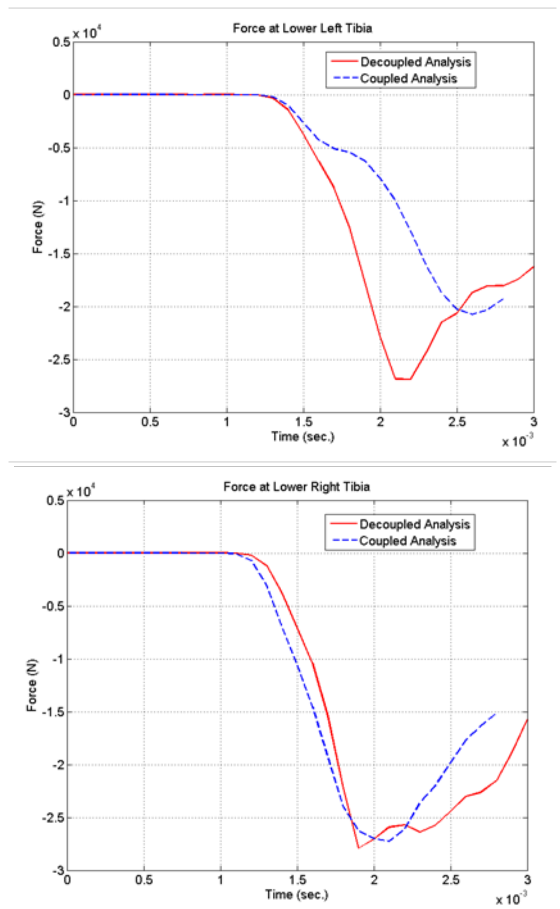

Figure 17. Forces developed in the lower left and right tibia of the dummy from a fully coupled and a decoupled blast simulation

The results for the velocity at a point on the floor which is between the left and the right heel of the ATD are presented in Figure 16, while results for the lower left and right tibia forces are presented in Figure 17. As it can be observed the results from the fully coupled analysis are overall very similar to the results from the decoupled analysis for the induced velocity of the deformation for the structure. The agreement is very good for the right lower tibia where the most severe response is expected due to the relative placement of the explosive with respect to the vehicle, and the coupled results are slightly lower for the force in the lower left tibia, since as expected in the decoupled analysis the vehicle experiences higher loads due to the lack of flexibility of the structure when evaluating the loads from the explosion. Given the level of correlation and the relative computational times, the decoupled approach is used in the design analysis for identifying blast mitigation strategies for reducing the loads in the lower left and right tibia.

BLAST MITIGATION STRATEGIES

Four different blast mitigation designs are considered by adding: an extra steel panel as a foot rest; a rail acting as a floor stiffener; placing RPF material in between the vehicle floor and the foot rest panel; or adding both a foot rest panel and a rail at the same time. These approaches and the associated results for the forces developed on the dummy are presented next. All four design alternatives are compared to the results from the baseline floor. All four design changes are implemented in the configuration with the sandwich floor that has 2cm of RPF placed in-between the outer and the inner floor panels. All results for the forces in the lower left and right tibia are compared to the forces created in the baseline floor configuration.

Design 1

A steel panel is added on top of the floor as a foot rest where the dummy's feet are placed. The thickness of the panel is 6 mm, and there is 2 cm gap between the panel and the floor.

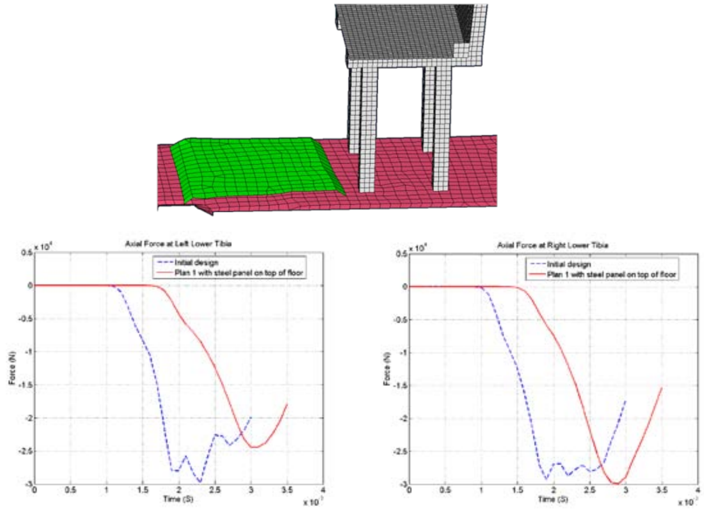

Figure 18. Steel panel added as a footrest; resulting forces on lower left and right tibia

Design 2

The same configuration with Design 1 but with RPF placed between the inner floor and the foot rest panel is analyzed. The configuration and the associated results are presented in Figure 19.

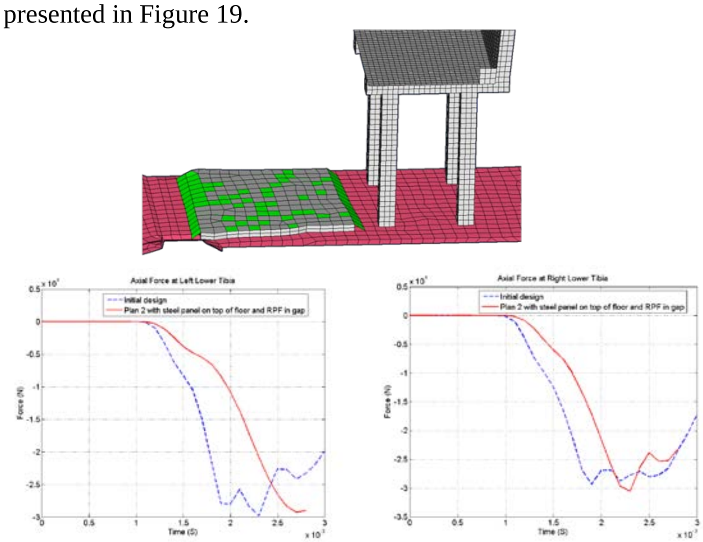

Figure 19. Steel panel added as a footrest with RPF filled between the floor and the panel; resulting forces on lower left and right tibia

Design 3

A steel rail with thickness of 10 mm is added on top of floor. The rail is attached at both ends to strengthen the vehicle floor, and to limit the global vertical motion at the area where dummy feet are placed. The configuration and the associated results are presented in Figure 20.

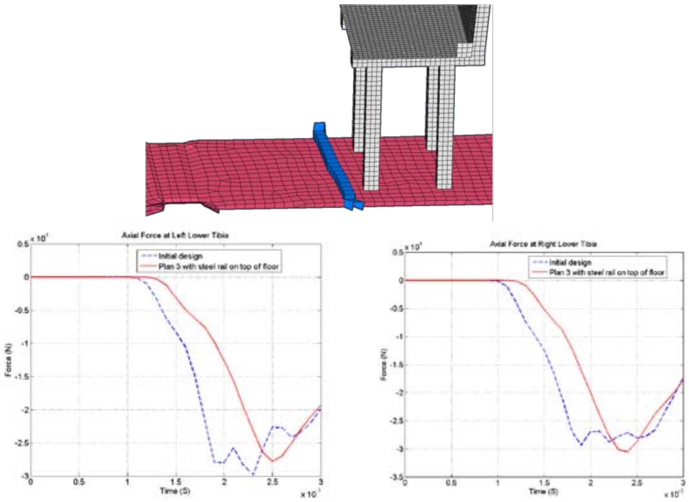

Figure 20. A steel rail added on top of the floor; resulting forces on lower left and right tibia

Design 4

The foot rest steel panel originating from Design 1 is combined with the steel rail stiffener introduced in Design 3 and they are both are placed together on top of the floor. The configuration and the associated results are presented in Figure 21.

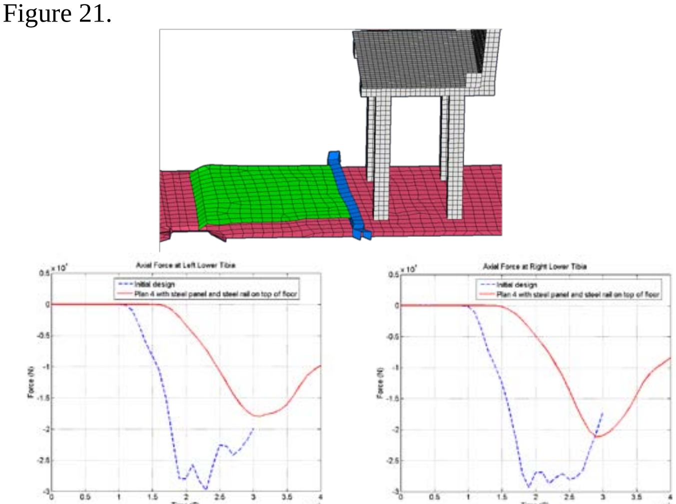

Figure 21. A steel rail added on top of the floor; resulting forces on lower left and right tibia

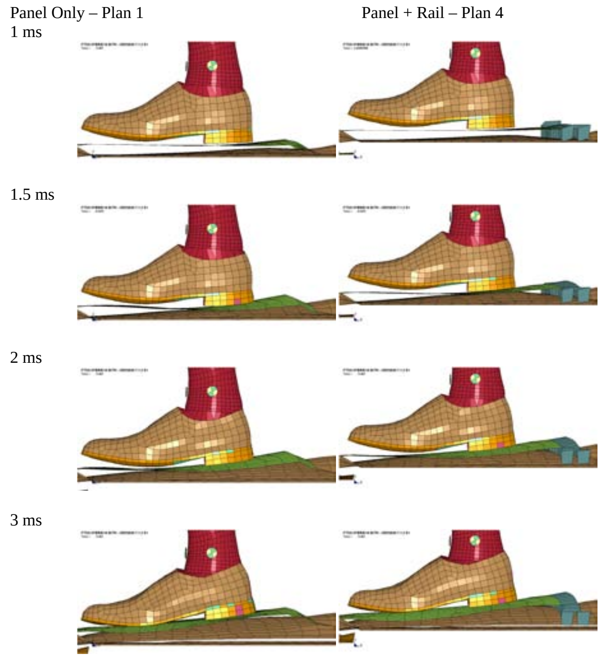

Figure 22. Comparative response of occupant between Design 1 and Design 4

Design 4 which has both the steel panel and the steel rail on top of the floor seems to reduce the tibia force most successfully, by about 30%. The rail helped the steel panel to maintain its shape and its clearance from the floor, therefore achieved the best isolation effect. Another observation is that due to the limited space in between the upper floor and the foot rest, placing RPF in the gap between the two did not absorb much energy; instead it compromised the isolation effect by transmitting the force more effectively. Further, by monitoring the movement of the floor, steel panel, and dummy feet, side by side for the panel only case (Design 1) and the panel plus rail case (Design 4) it can be observed that the amount of time that the feet are in contact with the panel is less for the case of the panel plus the rail configuration. The animations from the simulations were used to make this observation. In this paper, only a few frames are presented side-by-side in Figure 22. Design changes which limit the contact between the occupant and the vehicle are the ones which generate reduction in the loads developed in the members of an occupant.

CONCLUSIONS

The ability to simulate the response of a vehicle when it is subjected to the blast load from a buried off-centerline explosive charge is demonstrated, along with the capability to compute the loads which are developed in the members of an occupant. The BEST process enabled the explosive/soil/air/vehicle/occupant simulations. This is a process that has been validated in the past through comparisons to test data and was utilized in this paper for the analysis of the generic vehicle. Due to its computational efficiency, it was possible to study many different design changes in the vehicle structure in an effort to reduce the loads developed in the lower tibia of the occupant. This work demonstrates how simulation technology can be used for increasing an occupant's safety from blast loads.

AKNOWLEDGEMENTS

This study was funded under contract M67854-10-C-6523 from the USMC; TPOC: Joseph C Burns, and Patrick McMahon.

REFERENCES

[1] Gupta A.D., "Estimation of vehicle floor plate loading and response due to detonation of a mine shallow-buried in dry sand and wet turf," US Army Ground Vehicle Survivability Symposium, Monterey, CA, Mar. 29 – April 1, 1999.

[2] Bird R., "Protection of vehicles against landmines," Journal of Battlefield Technology, Vol. 4, No. 1, March 2001.

[3] Gupta A.D., "Modeling and analysis of a blast deflector for a tactical vehicle due to detonation of a mine buried in dry vs. saturated sand," US Army Ground Vehicle Survivability Symposium, 2002.

[4] Sun J., Vlahopoulos N., Stabryla T. J., Goetz R., Van De Velde R., "Blast event simulation for a structure subjected to a landmine explosion," 2006 SAE Congress, SAE Paper 2006-01-0931.

[5] Kingery C., and Bulmarsh G., "Airblast parameters from TNT spherical air burst and hemispherical surface burst," ARBRL-TR-02555, US Army Ballistic Research Laboratory, Aberdeen Proving Grounds, MD, 1984.

[6] Westine P.S., Morris B.L., Cox B.L., and Polch E.Z., "Development of computer program for floor plate response from land mine explosions," Technical report No. 13045, US Army Tank-Automotive Command, Warren, MI, 1985.

[7] McGlaun J.M., Thompson S.L., and Elrick M.G., "CTH: a three-dimensional shock wave physics code," Int. J. Impact Engng., Vol. 10, 1990, pp. 351-360.

[8] Bell R. L., Hertel Jr. E.S., "A domain decomposition scheme for Eulerian shock physics codes," CED-Vol. 6, High Performance Computing in Computational Dynamics, ASME International Congress and Exposition 1994, pp. 67-72.

[9] N. Vlahopoulos, G. Zhang, "Validation of a Simulation Process for Assessing the Response of a Vehicle and its Occupants to an Explosive Threat," 27th Army Science Conference, Orlando Fl, December 2010.

[10] Woodfin, R., "Rigid Polyurethane Foam (RPF) Technology for Countermine (Sea)Program - Phase 1," Sandia National Laboratories, Albuquerque, NM, 1997.

[11] Alba, Albert L., "Rigid Polyurethane Foam as a Breaching Technique for Anti-Personnel Mines", Master's Thesis, Naval Postgraduate School, Monterey, CA, December 1997.